J Solid State Electrochem (2008) 12:295–302
DOI 10.1007/s10008-007-0391-4

ORIGINAL PAPER

Lithium $AlPO_4$ composite polymer battery with nanostructured $LiMn_2O_4$ cathode

Zhumabay Bakenov · Masanobu Nakayama · Masataka Wakihara · Izumi Taniguchi

Received: 25 May 2007 / Revised: 3 July 2007 / Accepted: 13 July 2007 / Published online: 5 September 2007

Abstract The borate ester plasticized $AlPO_4$ composite solid polymer electrolytes (SPE) have been synthesized and studied as candidates for lithium polymer battery (LPB) application. The electrochemical and thermal properties of SPE were shown to be suitable for practical LPB. Nanostructured $LiMn_2O_4$ with spherical particles was synthesized via ultrasonic spray pyrolysis technique and has shown a superior performance to the one prepared via conventional methods as cathode for LPB. Furthermore, the $AlPO_4$ addition to the polymer electrolyte has improved the polymer battery performance. Based on the AC impedance spectroscopy data, the performance improvement was suggested as being due to the cathode/polymer electrolyte interface stabilization in the presence of $AlPO_4$. The Li/composite polymer electrolyte/nanostructured $LiMn_2O_4$ electrochemical cell showed stable cyclability during the various current density tests, and its performance was found to be quite acceptable for practical utilities at ambient temperature and showed remarkable improvements at 60 °C compared with the solid state reaction counterpart.

Keywords Lithium polymer batteries · Nanostructured lithium manganese oxide · Cathode/electrolyte interface

Z. Bakenov · M. Nakayama · M. Wakihara (✉)
Department of Applied Chemistry, Tokyo Institute of Technology,
2-12-1 Ookayama, Meguro-ku,
Tokyo 152-8552, Japan
e-mail: mwakihar@o.cc.titech.ac.jp

I. Taniguchi
Department of Chemical Engineering,
Tokyo Institute of Technology,
2–12–1 Ookayama, Meguro-ku,
Tokyo 152-8552, Japan

Introduction

Lithium-ion batteries (LIBs) are one of the great successes of modern materials electrochemistry [1]. Rechargeable LIBs with liquid electrolytes were developed and introduced into the market by Sony [2] in 1991. Despite its outstanding properties compared with other types of batteries such as nickel–cadmium and metal–hydride batteries, lithium batteries with liquid electrolytes suffer from safety problems due to flammability and possibility of the leakage of the electrolyte solution and application of high cost and toxic electrode materials.

The further development in the lithium battery field logically resulted in the development of lithium polymer batteries (LPBs) with solid polymer electrolytes (SPE) and plasticized or gel polymer electrolytes (GPE), which more attractive than liquid ones due to less possibility of electrolyte leakage and safer if abused. Along with improved safety characteristics, such polymer cells offer shape versatility, flexibility, and other advantages over liquid counterparts. Various kinds of polymer matrices were used for the GPE and SPE preparation [3]. Although the LPBs with GPE have been commercialized, the use of flammable organic solvents in GPE structure may cause battery 'flashing' under unexpected conditions. Therefore, the research for the SPE used LBPs is urgently demanded today. However, SPE suffers from a serious problem of low ionic conductivity at lower ambient temperatures. In our laboratory, the series of novel polymeric borate esters were tested as components of electrolytes for lithium ion batteries [4–6]. These systems were found to be high thermally and electrochemically stable polymer electrolytes with high ionic conductivity. In our recent study, this SPE was tested in the lithium battery with cobalt-substituted spinel $LiMn_{1.8}Co_{0.2}O_4$ prepared by solid state reaction

method [7, 8]. The cell exhibited acceptable cycle performance and storage stability.

Along with low ionic conductivity of SPE, the large solid–solid interfacial resistance between electrodes and electrolytes would be another technical difficulty to fabricate all-solid LPBs with sufficient rate performance. This limitation may be overcome by increasing the interfacial area; therefore, developing the fine- and uniform-grain size materials would be effective for the LPB technology. In addition, the replacement of high cost and toxic cobalt and nickel-containing electrodes by economically more reliable and environmentally friendly materials is the key of the further development of LIBs. Among the other candidates, lithium manganese spinel oxide $LiMn_2O_4$ is one of the most promising one due to the larger natural abundance of manganese sources and its ecological benign. However, the $LiMn_2O_4$ synthesized via common solid state reaction method suffers from drastic capacity fade upon cycling. Thus, the morphology and compound chemistry optimization are needed to fabricate the cathode materials for LPBs. In our previous works, we reported the ultrasonic spray pyrolysis synthesis of nanostructured spherical particles of lithium manganese oxide and its substituted derivatives [9–11]. The materials exhibited stable electrochemical performance at high rate charge–discharge operation in the cell with liquid non-aqueous electrolyte, which was superior to that of the solid state reaction counterpart. In our recent work [12], it was shown that non-substituted nanostructured $LiMn_2O_4$ with spherical particles exhibits a pronounced stability upon prolonged cycling at room temperature at high charge–discharge rates up to 10 °C, which is not reachable for non-doped lithium manganese spinel cathode synthesized via conventional methods. It was also shown [12] that the addition of aluminum phosphate to the electrolyte positively effects on the cell performance via the cathode–liquid electrolyte interface stabilization.

In the present work, we report the thermal and electrochemical properties of a polymeric borate ester plasticized $AlPO_4$ composite SPE, ambient and elevated temperature performance of lithium polymer cell with nanostructured lithium manganese oxide with spherical particles, and influence of the $AlPO_4$ additives on the Li/nanostructured $LiMn_2O_4$ all-solid polymer battery performance.

Experimental

All polymer samples were supplied from NOF (Japan). Figure 1 presents the structures of the components used for the SPE synthesis. The borate ester plasticized polymer electrolyte was obtained via the polymerization of the poly (ethylene glycol) methacrylates (PDE-600 and PME-400)

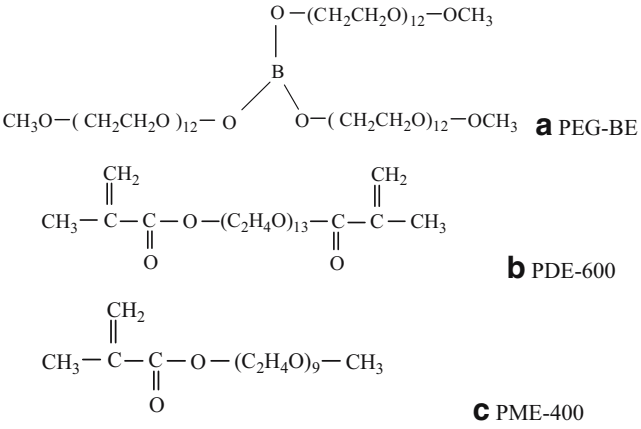

Fig. 1 Structural formulas of **a** borate ester and **b**, **c** poly(ethylene glycol) methacrylates

with addition of PEG-borate ester (PEG-BE), 1 mol kg^{-1} of $LiClO_4$ (Fluka). The weight ratio of the polymer components was PDE-600/PME-400/PEG-BE=15:15:70. The electrochemical properties of the pristine polymer electrolyte and the one with addition of 1, 5, and 10 wt% of $AlPO_4$ (Sigma-Aldrich) were studied in this work. Polymer electrolyte synthesis and sample preparation were carried out in a dry box filled with high purity argon. After stirring for 24 h, the viscous reacting mixture was transferred onto Teflon plate and polymerized using benzophenone (Sigma-Aldrich) as an initiator of the photopolymerization reaction. The polymer mixture was irradiated for 1 h by the ultraviolet light (254 nm) for the polymerization initiation. The resulting transparent and self-standing film of 1-mm thickness was used for the examination.

The ionic conductivity of the electrolyte was measured by AC impedance technique using Hewlett-Packard 4192A LF impedance analyzer. Thermal and electrochemical stability of the polymer systems were estimated, respectively, by thermogravimetric analysis (TGA) with TG/DTA-6300 (Seiko Instruments) apparatus and cyclic voltammetry using Solartron SI 1287 electrochemical interface.

Lithium manganese oxide $LiMn_2O_4$ was synthesized by the ultrasonic spray pyrolysis (USP) technique. The synthesis technique and the USP facility is described elsewhere [9–11]. The precursor solution of stoichiometric amounts of $LiNO_3$ and $Mn(NO_3)_2{\cdot}6H_2O$ (both 98% purity, Wako Pure Chemical Industries, Tokyo, Japan) in distilled water was atomized by the ultrasonic nebulizer (1.7 MHz, Omron, Model NE-U12) and carried to the laminar flow aerosol reactor, heated in air by an electric furnace at 800 °C, and converted into solid oxide particles through the process of evaporation of a solvent, precipitation of solute, drying, pyrolysis, and sintering. The resulting particles were collected by the electrostatic precipitator at 150 °C.

For all experiments, the total cation concentration was 0.90 mol/dm^3.

For comparison purposes, the lithium manganese oxide $LiMn_2O_4$ prepared by a solid state reaction of Li_2CO_3 and Mn_2O_3 at 700 °C in air was also used for the electrochemical measurements.

The X-ray diffraction (XRD, Phillips, PW1700) technique data have confirmed the single-phase cubic structure and $Fd\bar{3}m$ space group of the materials prepared by both methods. The inductively coupled plasma-optical emission spectroscopy (ICP-OES, Leeman Labs) has shown a good agreement between experimental and calculated values of the materials stoichiometry.

The electrodes were prepared by the deposition of the slurry of 70% active material ($LiMn_2O_4$), 20% of acetylene black conductor, and 10% polyvinylidene difluoride (PVDF) binder dissolved in NMP on an Al-foil. Electrochemical performance was investigated using a coin-type cell constructed as follows. The polymeric mixture of above composition with benzophenone photopolymerization initiator was placed on the surface of $LiMn_2O_4$ cathode and subjected to the UV radiation to initiate the polymerization. Then, several drops of polymeric mixture was added, and the Li-metal foil was placed on it, which thereafter irradiated for an hour more to accomplish the polymerization. The cell was sealed and galvanostatically charge/discharged between 3.5–4.2 V vs Li^+/Li on multi-channel battery testers (Hokuto Denko, HJ1010mSM8). To ensure the data reproducibility, two parallel cells of the same type were assembled.

Impedance spectroscopy of the polymer cells was conducted along with galvanostatic cycling of the cell using multi-channel potentiostat VMP3 (Bio-Logic SAS Co with EC-Lab® software) in the frequency range and voltage region from 50 mHz to 500 000 kHz and 3.5 to 4.2 V vs Li^+/Li, respectively. The AC impedance spectra fitting was made using ZSimpWin software (version 3.21, EChem Software).

Results and discussion

Characterization of polymer electrolytes

Both types of the polymer electrolytes—the pristine polymer and one with the addition of $AlPO_4$—showed satisfactory mechanical stability and adequate liquid component PEG-BE retention in the polymer matrix without any noticeable liquid trace on the surface.

Figure 2 shows the temperature dependence of the ionic conductivities of the polymer electrolytes conducted from 30 to 110 °C and represented in the Arrhenius plots. All polymer systems show a clear dependence of conductivity on temperature with the maximum value of 0.18 mS cm^{-1} at room temperature. This is mainly due to the increasing mobility of the Li-ions with temperature. The addition of $AlPO_4$ did not show remarkable effect on the ionic conductivity of the electrolyte. Addition of more than 1 wt% of $AlPO_4$ to the system led to the ionic conductivity decrease.

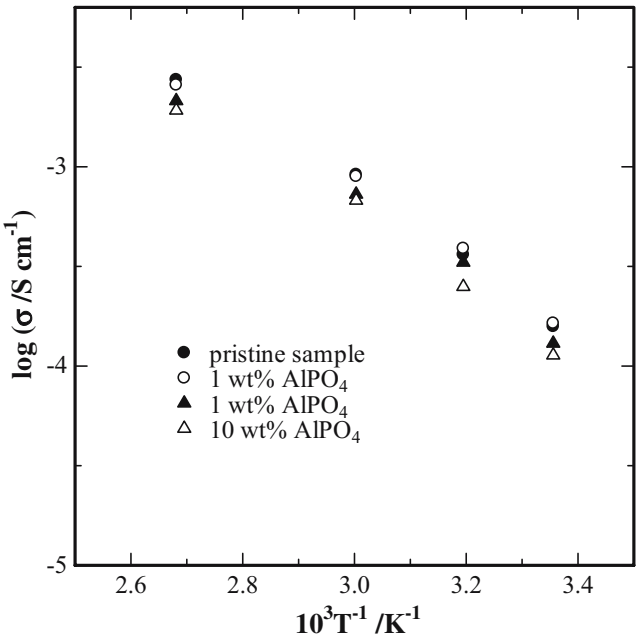

Fig. 2 Temperature dependence of ionic conductivity of PDE-600/PME-400/PEG-BE=15:15:70 polymer electrolytes, 1 mol kg^{-1} $LiClO_4$

The electrochemical stability is another important parameter to evaluate the viability of the polymer electrolytes in LPB, which was determined by cyclic voltammetry (CV). Figure 3 presents the CV data for the pristine and $AlPO_4$ added polymer electrolytes. It reveals that the electrochemical stability of both electrolytes is similar and shows an onset of the decomposition peak above 4.5 V in the anodic region during the first sweep, and for both electrolytes, the anodic oxidation starts at about 4.5 V. This implies that there is no decomposition of the electrolytes at the voltage region up to 4.4 V after the first cycle making them suitable for common LPBs. An addition of more than 1 wt% of $AlPO_4$ did not change the electrochemical window range of the polymer electrolyte (not shown). TG analysis data are presented in Fig. 4 and indicate that the thermal stability of polymer electrolytes has not been affected remarkably by the addition of $AlPO_4$. Therefore, it may be suggested that the addition of $AlPO_4$ into SPE does not cause remarkable bulk property change.

The data of the polymer electrolyte characterization have shown that the addition of 1 wt% of $AlPO_4$ may be considered as an optimal for the composite polymer electrolyte preparation. In the further studies, this composition was used to prepare polymer electrolyte battery.

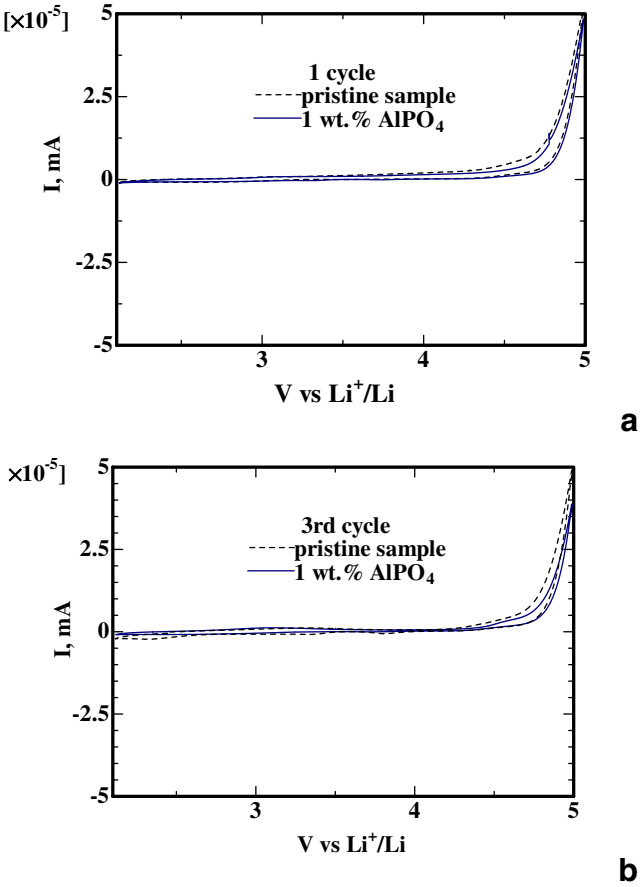

Fig. 3 CV plots of polymer electrolytes PDE-600/PME-400/PEG-BE= 15:15:70 wt%, 1 mol kg^{-1} $LiClO_4$, **a** 1st cycle, **b** 3rd cycle, 1 mV s^{-1}

Electrochemical performance of Li/polymer/$LiMn_2O_4$ cell: comparison of nanostructured and microstructured cathodes performance

The cyclability of LPB consisting of the nanostructured lithium manganese oxide spinel $LiMn_2O_4$ cathode and the SPE synthesized from PDE-600/PME-400/PEG-BE at 30 °C was examined. In our previous work [12], we reported that the nanostructured $LiMn_2O_4$ synthesized in the present study via USP technique has fine spherical particles and porous surface morphology. It was shown [12] that spherical particles of $LiMn_2O_4$ in the liquid electrolyte lithium cell exhibited established cycling performance and high rate capability.

For comparison purposes, in the present study, the electrochemical performance of the polymer cell with material prepared by solid state reaction (SSR) was also examined. Figure 5 shows the charge–discharge profiles of the nanostructured spherical $LiMn_2O_4$ prepared via USP method and its SSR counterpart in the Li/SPE/$LiMn_2O_4$ cell at 0.1C charge–discharge rate at 30 °C. It can be seen that both materials exhibit two intrinsic plateaus in the charge and discharge curves. The discharge capacities of the polymer cells reach about 80% of the theoretical capacity value. However, in comparison with the SSR material, the nanostructured material shows a slight decrease of discharge capacity loss at the initial cycles and lower charge–discharge polarization. The reduction of the capacity loss may be due to the higher electrochemical

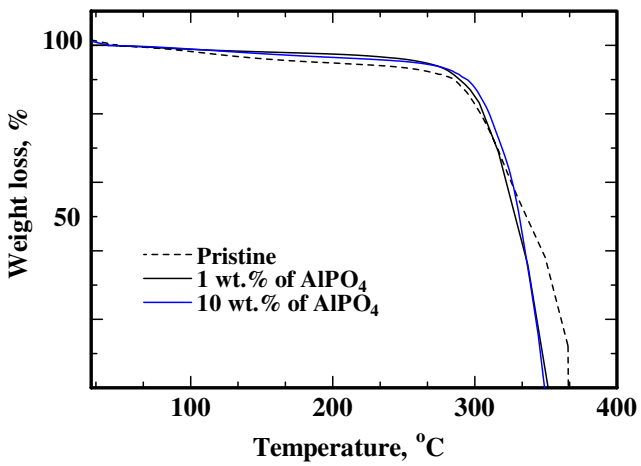

Fig. 4 Effect of addition of $AlPO_4$ to thermal stability of PDE-600/PME-400/PEG-BE=15:15:70 wt%, 1 mol kg^{-1} $LiClO_4$

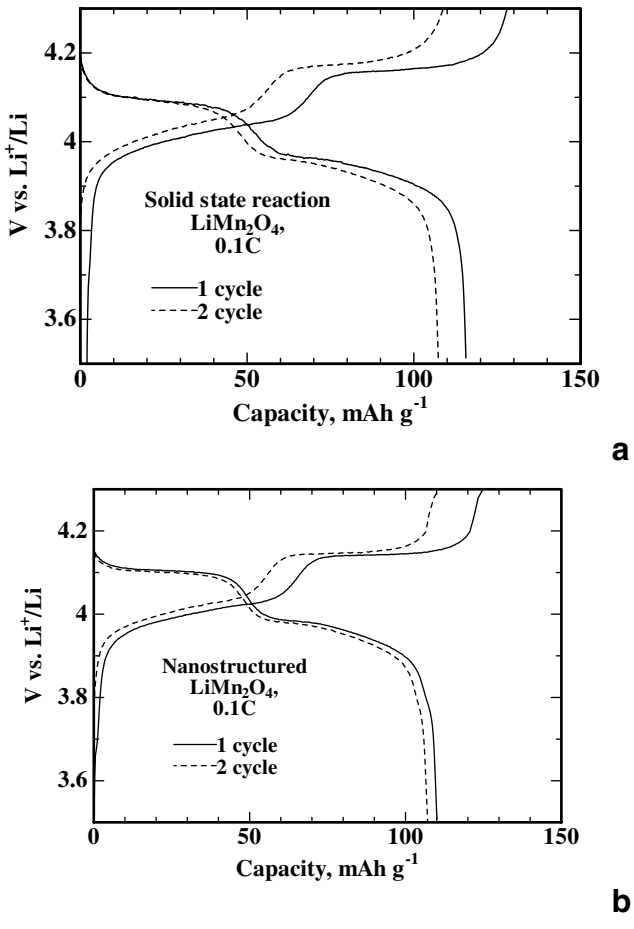

Fig. 5 Initial charge-discharge cycles profiles (0.1C rate and 30 °C) for the Li/SPE/$LiMn_2O_4$, **a** solid state reaction $LiMn_2O_4$, **b** ultrasonic spray pyrolysis nanostructured $LiMn_2O_4$

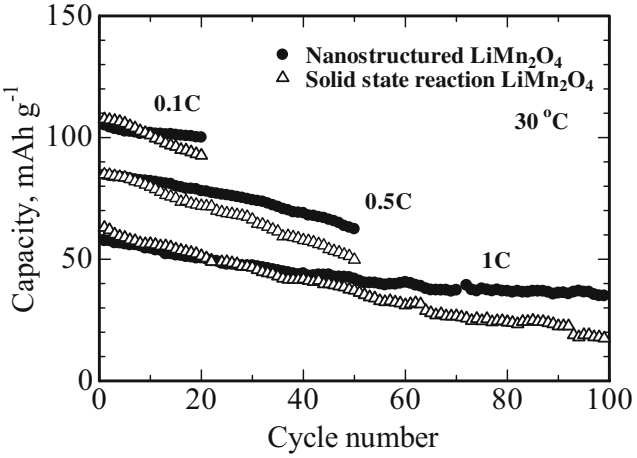

Fig. 6 Discharge capacity retention of $LiMn_2O_4$ prepared by different techniques in Li/SPE/$LiMn_2O_4$ lithium polymer battery, 30 °C

stability of the nanostructured $LiMn_2O_4$ compared with its SSR counterpart, as it was observed in the liquid electrolyte systems in our previous works [10–12]. The lower polarization during the electrochemical lithium insertion–removal into spherical particle material may be attributed to the short diffusion distance of Li^+ ions in the nanostructured electrode [13–15] compared with macrostructure of the SSR $LiMn_2O_4$. These conditions may favor the enhanced kinetics of the lithium cation transport and depress the total electrochemical reaction polarization.

Figure 6 presents the cyclability data of the materials prepared by two different techniques in the composite polymer battery at various charge–discharge rates. The results show superior performance of the nanostructured $LiMn_2O_4$ to the SSR counterpart for all charge–discharge conditions. The cell containing nanostructured electrode kept 61% of the initial specific capacity after 100 cycles at 1C rate, while for the SSR system, this value is about 30% of the starting capacity. The obtained data clearly show the

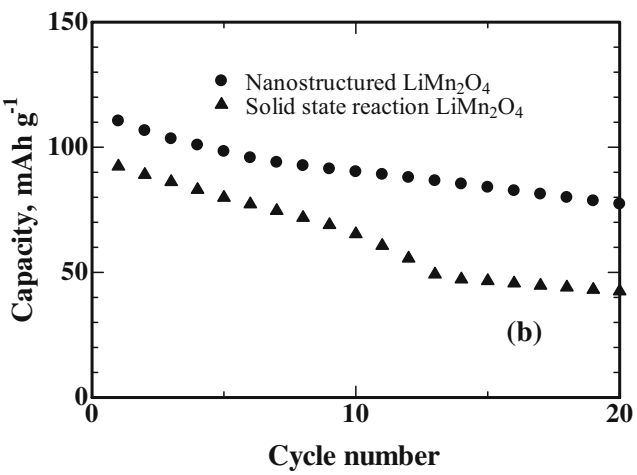

Fig. 7 Electrochemical performance of Li/SPE/$LiMn_2O_4$ cell at 60 °C, 1C

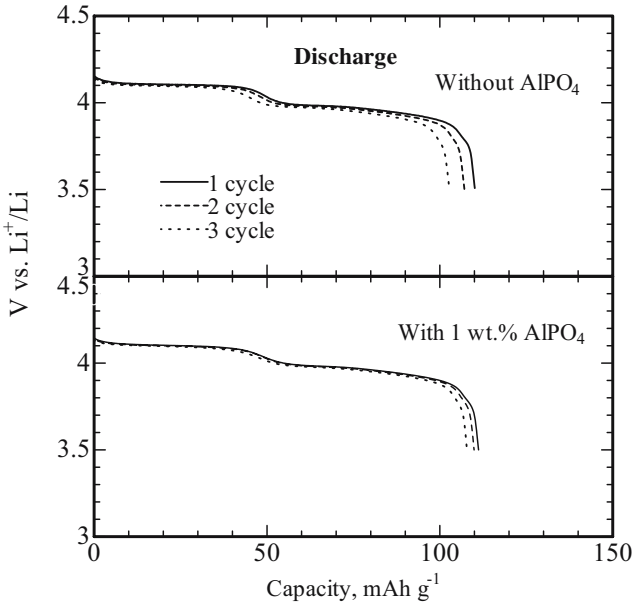

Fig. 8 Influence of the $AlPO_4$ electrolyte additives to the discharge properties of Li/SPE with 1 wt% of $AlPO_4$/$LiMn_2O_4$ cell (0.1C, 30 °C)

advantages of the spray pyrolysis technique for preparation of cathode materials for the LPB application with enhanced performance compared with the SSR method. This performance improvement could be attributed to the nanostructured features, dense spherical morphology, and homogeneous chemical composition [12] of the particles prepared via the spray pyrolysis technique.

Electrochemical performance of Li/polymer/$LiMn_2O_4$ cell: high temperature performance

The nanostructured $LiMn_2O_4$-based polymer battery performance at 60 °C was examined. Figure 7 exhibits comparative data of the high temperature cyclability of

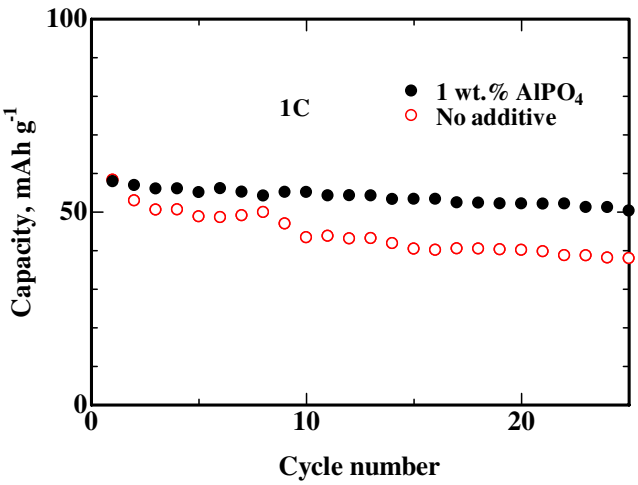

Fig. 9 Influence of the $AlPO_4$ additives to room temperature performance of the Li/SPE/nanostructured $LiMn_2O_4$ cell (1C, 30 °C)

nanostructured and SSR made $LiMn_2O_4$ at 1C charge–discharge rate. It is clearly seen that the elevated temperature performance of the nanostructured cathode is remarkably enhanced and has smaller capacity decay compared with the SSR counterpart. Figure 7 also shows that at the elevated temperature conditions, the cells exhibits almost twice higher value of the initial discharge capacity than at ambient temperature conditions (Figs. 5, 6). This phenomenon would be attributed to the enhancement of the Li^+ ion transport conditions at the elevated temperature, which is provided by more polymer matrix flexibility and adequate ionic conductivity at higher temperature.

In general, it is reported in the literature that the phenomenon of poor high temperature cyclability of the $LiMn_2O_4$ is attributed mainly to its inherent properties, which lead to Mn dissolution [18], and decomposition of the electrolyte at high-voltage regions [16]. Although the results of the current study show the similar effect of temperature on

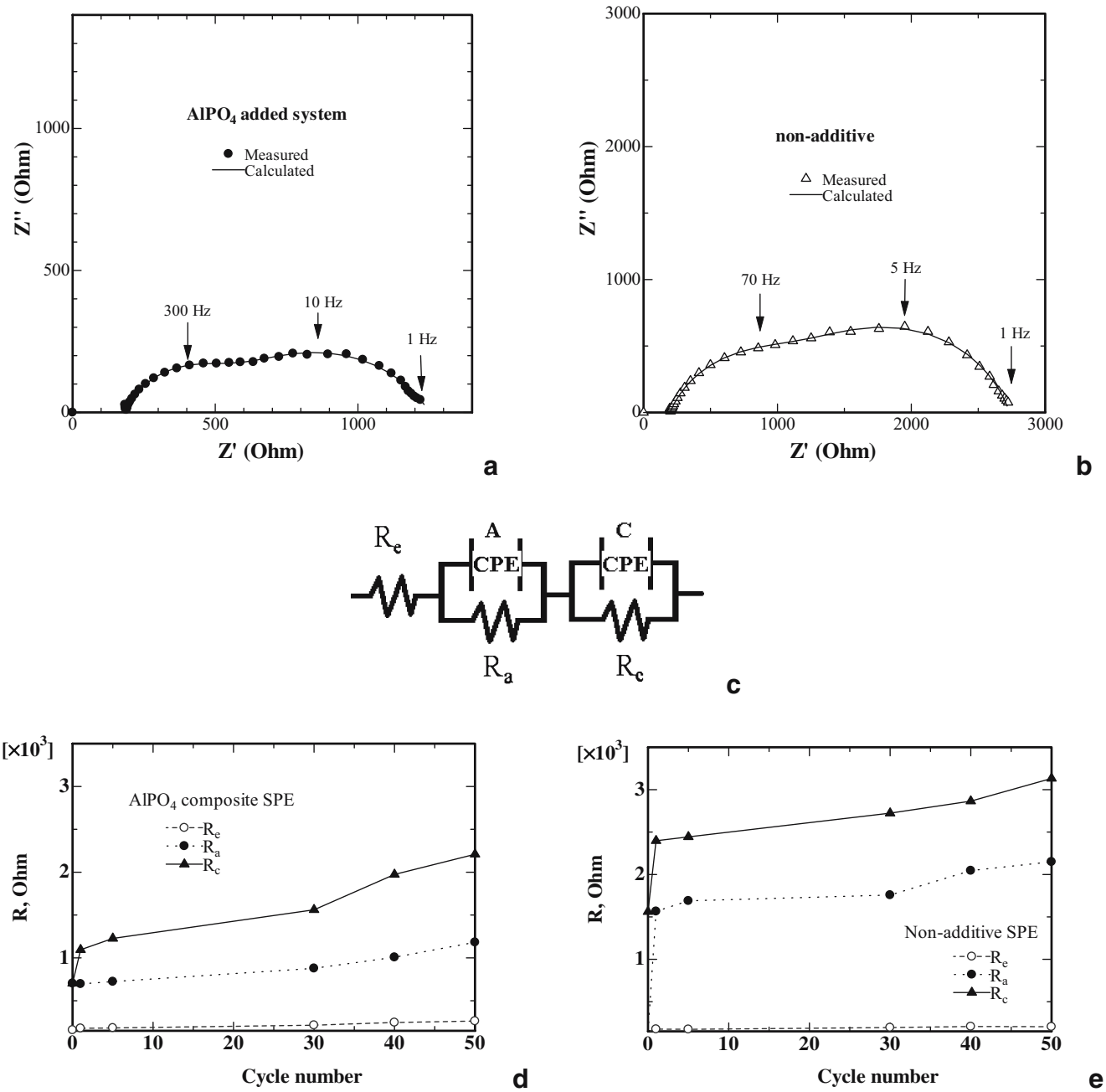

Fig. 10 **a**, **b** AC impedance spectra of the Li/SPE/nanostructured $LiMn_2O_4$ cell. *Fitting lines* show calculated results from equivalent circuit (**c**); impedance components dependence on cycle number, **d** $AlPO_4$ added LPB, **e** non-additive LPB

the nanostructured $LiMn_2O_4$ performance as a cathode for LPBs, there is a remarkable improvement of its performance compared with the microstructured SSR $LiMn_2O_4$.

Further works are considered for the optimization of the cathode material for the high temperature operation.

Electrochemical performance of Li/polymer/$LiMn_2O_4$ cell: influence of the $AlPO_4$ addition on the cathodes performance

The influence of the $AlPO_4$ additives to the LPB performance was investigated. Figure 8 shows the comparison of the electrochemical performance of the nanostructured $LiMn_2O_4$ lithium cell with the aluminum phosphate added polymer electrolyte and the one without additive. One can see that both cells exhibit the discharge profiles with two plateaus inherent for the $LiMn_2O_4$ spinel cathodes in the prolonged and flat manner. The data show that the $AlPO_4$-containing cell has enhanced capacity retention compared with the cell without the additive.

Figure 9 illustrates the effect of $AlPO_4$ addition to the discharge capacity retention of LPB with nanostructured $LiMn_2O_4$ cathode at 30 °C and higher 1C charge-discharge rate. No marked difference was observed at first discharge voltage profile for both samples, while one can see the continuous degradation of discharge capacity in the LPB without $AlPO_4$ at following cycles. It can be seen that the LPB with aluminum phosphate additive exhibits more stable electrochemical performance than the additive free battery. The following mechanisms of the additive effect may be considered. The first is the affect on the electrochemical performance of the cell by removing residual amounts of water by the $AlPO_4$ particles added to the polymer electrolyte. Another suggested reason of the performance enhancement of the additive containing LPB may be the electrolyte–electrode interface stabilization in the presence of $AlPO_4$, as it was observed in the case of liquid electrolyte lithium battery [12, 19–20].

AC impedance technique [16] is helpful for determining the surface modification effects at the electrode and electrolyte interface. The AC impedance spectra of the cells with nanostructured cathode were measured before cycling and along with galvanostatic cycling at the charged and discharged states of the cell, respectively. The impedance development for both charged and discharged states had the same trend. Figure 10 presents the impedance plots of the LPB with $AlPO_4$ addition and without the additive at its charged state and the dependence of the impedance components on cycle number.

Figure 10a,b show typical experimental Cole–Cole plots for both the $AlPO_4$ added and the additive-free cells with two depressed semicircles along with the calculated curves from the equivalent electric circuit, presented in Fig. 10c. A constant phase elements A-CPE and C-CPE represent the double layer and passivation capacitances on the anode and cathode surfaces, respectively. One can see that the measured data agree well with the fitting using the proposed equivalent circuit. Figure 10d, e presents the dependence of the impedance spectra components upon cycling, calculated using the equivalent circuit. The high frequency intercept at the Z'-axis corresponds to the electrolyte resistance, R_e. This component of the impedance spectra is almost unchanged during the cell operation (see Fig. 10d,e). In the middle frequency part the R_e is followed by a semicircle, which is attributed to the polymer electrolyte (SPE)/lithium interface impedance, R_a [16, 17], and the R_a diameter is noticeably smaller for the $AlPO_4$ added cell. The semicircle in lower frequency (LF) range would be assigned to the SPE/cathode interfacial resistance, R_c [16]. In comparison with other impedance components, the value of R_c (diameter of the LF arc) enlarges upon the cycling. One can see from Fig. 10d,e data that the $AlPO_4$ containing LPB keeps smaller values of R_c compared with the $AlPO_4$ additive free system. This difference further enlarges with cycling, indicating better stability at $AlPO_4$ added SPE| cathode interface. This behavior is obviously correlated with the electrochemical performances for both the additive containing and additive-free cells as shown in Figs. 8 and 9. In other words, the poorer performance of the $AlPO_4$ additive-free polymer cell would be correlated with the interfacial impedance development during the cell operation. These results of comparative AC impedance spectra for the studied cells strongly suggest that there is a clear effect of $AlPO_4$ additive to the cell performance due to the improvement of the impedance behavior at the electrode–electrolyte interface in the presence of $AlPO_4$. It may be suggested that this electrolyte additive leads to the improved stability of the electrode surface by the stable

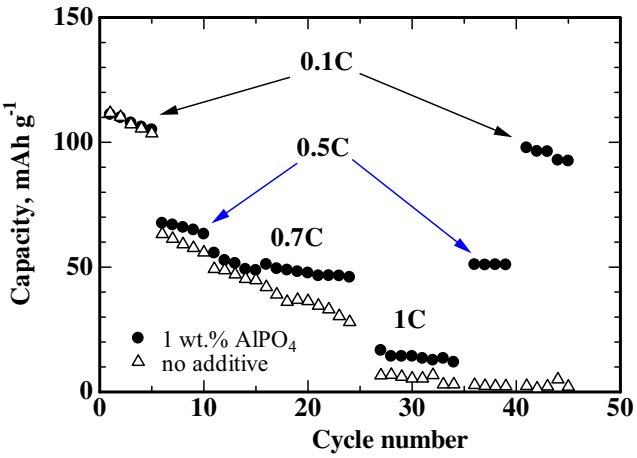

Fig. 11 Influence of the charge–discharge rates variation on discharge capacity of the polymeric cell Li/SPE with 1 wt% of $AlPO_4$/nanostructured $LiMn_2O_4$, 30 °C

interface formation, which prevents the further degradation of the electrode upon cycling, and may play an important role in the cell performance improvement.

The electrochemical performance of the Li/nanostructured $LiMn_2O_4$ polymer battery with/without the addition of $AlPO_4$ was tested by the application of variable current densities to the given electrochemical cell. The cell was initially cycled at low current density of 0.1C, then the charge–discharge rate was increased. After cycling for various rates up to 1C, the same cell was returned to the initial cycling conditions (0.1C). If cell gains its initial capacity, one may suggest that there is no critical destructive changes in the polymer cell upon variable and high rate operation. Figure 11 shows an example of such tests. It can be seen that after four step changes in the charge–discharge rates and cycling at the initial conditions of 0.1C, the cell with the addition of $AlPO_4$ reached about 90% of its starting capacity, while the pristine cell could not be recovered after being cycled at higher electric current. This fact allows the suggestion that the addition of $AlPO_4$ improves the cell stability during the changes in the electric current up to 1C and may provide additional safety for the cases of the fluctuation of the operation electric current.

Conclusion

The electrochemical performance of a novel rechargeable polymer battery based on nanostructured $LiMn_2O_4$ with spherical particles and PEGBE-PEG methacrylates-$AlPO_4$ composite electrolyte was studied. The comparative study of the electrochemical performance of lithium manganese spinel oxides prepared by the USP technique and SSR has shown a superior performance of the nanostructured $LiMn_2O_4$ prepared by USP to that of the SSR counterpart. The AC impedance studies data have shown a remarkable influence of the $AlPO_4$ additive on the polymer battery impedance. The impedance development was suppressed in the presence of aluminum phosphate. These data are in good correspondence with the battery cycling performance, where the $AlPO_4$ added cell showed enhanced cycling stability compared with the cell without the aluminum phosphate additive. The lithium cells with $AlPO_4$ composite polymer electrolyte at 60 °C have exhibited almost twice higher discharge capacity compared with ambient temperatures. The nanostructured $LiMn_2O_4$ with spherical particles showed the superior elevated temperature performance to the SSR counterpart as cathode for LPBs.

References

1. Aricò AS, Bruce P, Scrosati B, Tarascon JM, van Schalkwijk W (2005) Nature Materials 4:366
2. Ozawa K (1994) Solid State Ionics 69:212
3. Nishi Y (2002) Lithium-ion secondary batteries with gelled polymer electrolytes. In: van Schalkwijk WA, Scrosati B (eds) Advances in lithium-ion batteries. Kluwer, New York, pp 233–250
4. Kato Y, Yokoyama S, Ikuta H, Uchimoto Y, Wakihara M (2001) Electrochem Commun 3:128
5. Kato Y, Hasumi H, Yokoyama S, Yabe T, Ikuta H, Uchimoto Y, Wakihara M (2002) Solid State Ionics 150:355
6. Saito M, Ikuta H, Uchimoto Y, Wakihara M, Yokoyama S, Yabe T, Yamamoto M (2003) J Electrochem Soc 150(4):A477
7. Kottegoda IRM, Bakenov Zh, Ikuta H, Uchimoto Y, Wakihara M (2005) Electrochem Solid-State Lett 8(1):A30
8. Kottegoda IRM, Bakenov Zh, Ikuta H, Uchimoto Y, Wakihara M (2005) J Electrochem Soc 152(8):A1533
9. Bakenov Zh, Taniguchi I (2005) Solid State Ionics 176:1027
10. Taniguchi I, Bakenov Zh (2005) Powder Technology 159:55
11. Taniguchi I (2005) Material Chem Phys 92:172
12. Bakenov Zh, Wakihara M, Taniguchi I (2007) J Solid State Electrochem (in press). DOI 10.1007/s10008-007-0337-x
13. Im D, Manthiram A (2003) J Electrochem Soc 150:A742
14. Im D, Manthiram A (2002) J Electrochem Soc 149:A1001
15. Li N, Patrissi CJ, Che G, Martin CR (2000) J Electrochem Soc 147:2044
16. Seki S, Kobayashi Y, Miyashiro H, Yamanaka A, Mita Y, Iwahori T (2005) J Power Sources 146:741
17. Seki S, Kobayashi Y, Miyashiro H, Mita Y, Iwahori T (2005) Chem Mater 17:2041
18. Ma S, Noguchi N, Yoshio M (2001) J Power Sources 97–98:385
19. Kobayashi Y, Seki S, Yamanaka A, Miyashiro H, Mita Y, Iwahori T (2005) J Power Sources 146:719
20. Miyashiro H, Kobayashi Y, Seki S, Mita Y, Usami A, Nakayama M, Wakihara M (2005) Chem Mater 17:5603